RSC Advances

Polysaccharide Stabilized Nanoparticles for Deacidification and Strengthening of Paper

Journal:	*RSC Advances*
Manuscript ID:	RA-ART-11-2014-015153.R3
Article Type:	Paper
Date Submitted by the Author:	14-Mar-2015
Complete List of Authors:	Amornkitbamrung, Lunjakorn; University of Graz, Institute of chemistry Mohan, Tamilselvan; University of Graz, Institute of chemistry Hribernik, Silvo; University of Maribor, Institute of Engineering Design and Materials, Laboratory for the Characterization and Processing of Polymers Reichel, Victoria; Max Planck Institute of Colloids and Interfaces, Department of Biomaterials Faivre, Damien; Max Planck Institute of Colloids and Interfaces, Department of Biomaterials Gregorova, Adriana; Graz University of Technology, Institute for Chemistry and Technology of Materials Engel, Patricia; Donau-Universität Krems, European Research Centre for Book and Paper Conservation-Restoration Kargl, Rupert; University of Maribor, Institute of Engineering Design and Materials, Laboratory for the Characterization and Processing of Polymers Ribitsch, Volker; University of Graz, Institute of Chemistry

Polysaccharide Stabilized Nanoparticles for Deacidification and Strengthening of Paper

Lunjakorn Amornkitbamrung[†], Tamilselvan Mohan[†], Silvo Hribernik[‡], Victoria Reichel[ζ], Damien Faivre[ζ], Adriana Gregorova[$], Patricia Engel,[β] Rupert Kargl[‡], Volker Ribitsch[†]*

[†]Institute of Chemistry, University of Graz, Heinrichstraße 28, AT 8010 Graz, Austria.

[‡]Faculty of Mechanical Engineering, Institute for Engineering Materials and Design, University of Maribor, Smetanova 17, 2000 Maribor, Slovenia.

[ζ]Department of Biomaterials, Max Planck Institute of Colloids and Interfaces, Potsdam-Golm Science Park Am Mühlenberg 1 OT Golm, DE 14469 Potsdam, Germany

[$]Institute for Chemistry and Technology of Materials, Graz University of Technology, Stremayrgasse 9, AT 8010 Graz, Austria

[β]European Research Centre for Book and Paper Conservation-Restoration, Donau-Universität Krems, Dr.-Karl-Dorrek-Straße 30, 3500 Krems, Austria

Corresponding Author

*tamilselvan.mohan@uni-graz.at
Karl-Franzens-University Graz
Institute of Chemistry
Heinrichstraße 28/III
A-8010 Graz/Austria
Phone: 0043 316 380 5413

ABSTRACT

This paper reports an investigation on the use of a highly stable colloidal organic dispersion consisting of a polysaccharide derivative and alkaline nanoparticles for the simultaneous deacidification and strengthening of aged historical wood pulp (HWP) and new paper. Colloidal dispersions of $Mg(OH)_2$ nanoparticles (size *ca.* 150 nm) stabilized by trimethylsilyl cellulose (TMSC) in hexamethyldisiloxane (HMDSO) are employed for paper treatments. The influence of the polymer shell on the morphology of particles and the stability of the dispersions, and polymer-particles interactions are examined. A correlation between the polymer concentration and stability of the nanoparticles is established. The influence of the particle/polymer coatings on the optical appearance, the pH, the alkaline reserve and the strength of paper is investigated by pH-measurements of cold-extracts, back-titrations, artificial aging and mechanical testing. Infrared spectroscopy confirmed the irreversible deposition of nanoparticles and TMSC on the paper. The surfaces are evenly coated as confirmed by electron microscopy and contact angle measurements, and the coating does not change the optical appearance of paper. Results from pH measurements and back-titrations have proven neutralization of acids and an alkaline reserve of 60 meq $[OH^-]$/100 g of paper before aging and 41 meq $[OH^-]$/100 g of paper after aging. Upon aging TMSC is hydrolyzed into cellulose and the coated paper exhibits a 20% higher tensile strength than uncoated paper.

KEYWORDS: Magnesium Hydroxide, Nanoparticles, trimethylsilyl cellulose, deacidification, strengthening, alkaline reserve

1. INTRODUCTION

Paper has been the most significant carrier of written information for many centuries. The deterioration of paper based items such as books and other written documents over time is a serious problem for libraries, archives and conservators around the world. A main cause of deterioration is the acidity generated upon natural aging.[1-3] From a material perspective cellulose is the main component and represents the largest number of paper based items.[4, 5] It is well known that the dominant chemical reaction that occurs during aging of paper is the acid-catalyzed hydrolysis of cellulose.[2, 6] Acid-hydrolysis leads to an irreversible depolymerisation of cellulose chains and consequently accounts for a substantial loss of mechanical strength.[2, 7, 8] The process of complete neutralization of acidity in paper and deposition of alkaline components is referred to as 'deacidification'. Up to now, many deacidification methods have been developed to eliminate the detrimental effects of acidity in paper and to simultaneously increase mechanical strength.[1, 3, 9-12] Despites other existing methods, aqueous solutions and dispersions of alkaline metal hydroxides such as calcium and magnesium have been employed for several decades owing to their high compatibility.[13, 14] Recently, a non-aqueous process of alcoholic (*e.g.* ethanol and propanol) dispersions of alkaline nanoparticles (NPs) such as calcium and magnesium hydroxide has been explored for papers, manuscript and archeological woods.[1, 9, 10, 15] These dispersions showed high stability and compatibility and are easy to handle. The nanoparticles cause a sufficient alkaline environment (pH 6-7.5) by turning into mild alkaline species *i.e.* carbonates. Nonetheless, apolar organic solvents were also used in a variety of processes employing soluble alkaline substances. One of these solvents is hexamethyldisiloxane (HMDSO) used in the well-established Battelle process.[16] HMDSO is inert, exhibits low surface tension (15.9 mN m^{-1}) and allowing a sufficient wetting of paper. More importantly it causes a better dimensional stability of paper after treatment due to a very low swelling capacity for cellulose fibers.[16, 17]

Recently this solvent was used together with soluble amine-bearing siloxanes for the deacidification and strengthening of paper.[3, 11, 12] Although, the above mentioned deacidification methods are versatile in one or the other way, a suitable approach to overcome some drawbacks is to employ substances that are fully compatible with the treated materials. In this context, a combination of silylated polysaccharides such as trimethylsilyl cellulose (TMSC) and alkaline nanoparticles *i.e.* $Mg(OH)_2$ could be feasible. TMSC is hydrophobic, soluble in a wide range of organic solvents, and its surface shows a lower water wettability and surface free energy. It has been the focus of cellulose model surface preparation, and was used for the preparation of nanoparticles.[18-22] On the other hand, $Mg(OH)_2$ NPs with a narrow size distribution are commercially available, and exhibit many advantages such as a high deacidification efficiency, economic benefits, simplicity of operations and compatibility with natural materials.[9, 23, 24] The deacidification of acid papers using $Mg(OH)_2$ NPs is not new and it is already well-established in the pioneering work of Giorgi et al.[23, 24] In their work $Mg(OH)_2$ NPs stabilized in alcohol are successfully applied for the deacidification and providing an additional alkaline reserve. While $Mg(OH)_2$ can be dispersed in some alcohols,[9, 23] it is very difficult to disperse them in very apolar organic solvents such as toluene without an additional stabilizer. In such cases, organosoluble TMSC can be used as it imparts a better dispersibility and colloidal stability to nanoparticles due to the hydrophobic trimethylsilyl (TMS) groups and steric repulsion of adsorbed hydrophobic polymer chains.[22] Moreover, the use of TMSC for deacidification treatment could act as a strengthening component for cellulose fibers in paper.

The aim of this work was therefore to develop an efficient deacidification treatment based on a TMSC stabilized colloidal dispersion of alkaline $Mg(OH)_2$ NPs in HMDSO. The kinetic stability, size and morphology of these particles were investigated by UV-Vis spectroscopy, dynamic light scattering (DLS) and transmission electron microscopy (TEM). Filter and

acidic historical wood pulp (HWP) paper were coated with the dispersions. The successful coating of the nanoparticles and long-term effect of the deacidifying treatments were examined by artificial aging tests and studied in detail by electron microscope, colorimetric, infrared (IR) spectroscopy, wettability, alkaline reserve titrations, pH measurements and testing of the mechanical strength.

2. EXPERIMENTAL SECTION

2.1 Materials and methods

Magnesium hydroxide nanoparticles ($Mg(OH)_2$, 99.8%, particle size < 100 nm) and hexamethyldisiloxane (HMDSO, 98%) were purchased from Sigma-Aldrich, Austria. Trimethylsilyl cellulose (TMSC, $DS_{TMS:}$ 2.8, M_w:149,000 g mol^{-1}, derived from Avicel PH-101) for the stabilization of $Mg(OH)_2$ nanoparticles in HMDSO was purchased from Thüringisches Institut für Textil- und Kunststoff-Forschung e.V. (TITK, Rudolstadt, Germany). Two kinds of paper samples were used for the deacidification experiments: 115A - type filter paper (made of 100% cellulose, ash content = 0.06 %, surface weight = 80 g m^{-2}) from Carl Roth, Germany and historical wood pulp (HWP, made of 50% ground wood pulp and 50% chemical pulp, with high lignin content) papers collected from books printed in 1840. All chemicals and materials were used without any purification. Milli-Q (18.2 M Ω cm at 25°C) water from a Millipore water purification system (Billerica, USA) was used for contact angle, pH and alkaline reserve measurements.

2.2. Stabilization of $Mg(OH)_2$ NPs in TMSC

1 g of $Mg(OH)_2$ NPs was added to 0.1, 0.5 and 2 g of TMSC (dissolved in 100 mL of HMDSO). The mixtures were sonicated (Elmasonic S40, Elma, Germany) for 30 min at 25°C

to obtain a stable colloidal dispersion of TMSC-$Mg(OH)_2$ NPs. The TMSC stabilized $Mg(OH)_2$ NPs were always prepared freshly prior to the impregnation of paper.

2.3 Coating and peeling of paper

Coating experiments: A simple dip coating procedure was adapted to deposit the TMSC and the TMSC/$Mg(OH)_2$ NPs mixture on paper. Briefly, the papers were cut into 4 x 5 cm^2. For coating, 1 g of paper (6 paper sheets) were immersed into 200 mL of TMSC-$Mg(OH)_2$ dispersion ($Mg(OH)_2$: 1 % (w/v), TMSC: 2 % (w/v)) for 30 min. The mixtures were stirred constantly during the coating process. For comparison, the paper sheets were impregnated in TMSC solution and in HMDSO under the same condition as described above. Afterwards, the paper sheets were taken out and vacuum dried (0 bar) at 25 ºC for 24 h.

In addition particles concentration of 0.0625 and 0.25% (w/v) were employed for coating of filter and HWP papers in order to tune the final pH and alkaline reserve (AR) of deacidified papers.

Peeling experiments: To verify the penetration of TMSC-$Mg(OH)_2$ NPs or its aggregates into the inner paper structure we conducted a peeling experiments. For this purpose, HWP papers (uncoated and coated, 4 x 5 cm^2) were chosen. Briefly, an adhesive tape was placed on the paper surface (front side), pressed for 1 min and removed afterwards. Similarly the materials were removed from other side (back) of the paper. This procedure was repeated five times. For analysis, the materials that remained after peeling (*i.e.* materials, not attached to the adhesive tapes) were used.

2.4 Accelerated aging of paper

Paper sheets were aged in order to accelerate the degradation of cellulose following a protocol published elsewhere.[10] For that purpose, 10 g of paper sheets (coated/uncoated) were placed in a closed desiccator containing 200 mL water saturated with NaCl to maintain the humidity

at 75% RH. The temperature for aging was set to 80ºC. The papers were aged under these conditions for 14 days. After aging, the papers were vacuum dried (0 bar) at 25ºC and conditioned at 23ºC and 65% RH for 24 h.

3. ANALYTICAL METHODS

3.1 UV-Vis spectroscopy. The colloidal stability of $Mg(OH)_2$ NPs in HMDSO with and without TMSC was investigated by UV-Vis spectroscopy. $Mg(OH)_2$ (1 g) was added to 100 mL of HMDSO or TMSC/HMDSO polymer (0.1, 0.5 and 2 g) and subjected to ultrasonication for 30 min. The kinetic stability of the samples was determined by transmission measurements at a wavelength of λ = 600 nm (optical path length of 10 mm). The cuvette was capped to avoid a loss of solvent during the measurements.

3.2 Dynamic light scattering (DLS). The nanoparticles mean hydrodynamic diameter was determined by DLS using a Brookhaven Instruments ZetaPlus zeta-potential Analyzer (wavelength: 657 nm, scattering angle: 90°). The samples were diluted with HMDSO ($Mg(OH)_2$: 0.01% (w/v), TMSC: 0.02% (w/v)). Mean particle diameters were approximated as the effective (z -average) diameters from the bimodal size distribution. The width of the distribution was achieved using the Non-Negatively constrained Least Squares (NNLS) method, presuming spherical particle shape and log-normal size distribution.[25] The measurements were repeated five times.

3.3 Transmission electron microscope (TEM). The morphology and particle size distribution of $Mg(OH)_2$ and TMSC stabilized $Mg(OH)_2$ NPs were analyzed using TEM. For TEM analysis, the samples were prepared by dropping 10 µL of dispersion (sonicated for 10 min) on 400 mesh carbon coated copper grids (purchased from Plano GmbH, Germany),

followed by drying at room temperature. The samples were diluted with HMDSO in the same way as above (section 3.2). The TEM images were obtained at 120 kV with a ZEISS EM912 at a magnification of 4000-10000. The particle size was calculated by analyzing the TEM images using the software Image J1.47 and at least 100 particles were chosen for analysis.

3.4 Field emission scanning electron microscopy (FESEM). The morphology of uncoated, coated and peeled paper samples were analyzed by FESEM. A Carl Zeiss FE-SEM SUPRA 35 VP electron microscope was used. The images were recorded with an acceleration voltage of 1 kV. The chemical compositions of coated/uncoated paper were examined using an Energy dispersive X-ray (EDX) detector (model OXFORD INCA 200, Oxford Instruments Germany, Wiesbaden, Germany). The EDX detector is equipped with a liquid nitrogen cooled X-ray detector (Si(Li) – silicon with lithium) having 10 mm^2 crystal area. The working distance for the EDX detector was 8.5 mm and the electron energy (acceleration voltage) was 10 keV. The paper samples were mounted on sample holders and no sputtering on the sample surfaces was performed. For the elemental mapping, a 10 nm gold layer was sputtered on the sample surface.

3.5 Colorimetric measurements. Color measurements of uncoated, coated and aged papers (4 x 4 cm^2) were determined in reflectance mode (spectral range 400-700 nm in 10 nm steps) using a Spectraflash SF 600 PLUS spectrophotometer (Datacolor) equipped with an integrating sphere. All experiments were conducted on at least three independent samples and on both sides of the sample surface, and an average value was obtained. The sample spot size of 3 x 3 cm^2 was used for the measurement. The color coordinate values (L, a, b)* were calculated in the CIE*LAB1976 Color System, with a D65 standard illuminant and 10° standard observer. D65 (LAV/Spec. Incl., d/8, D65/10°). On the basis of measured CIE (L, a,

b)* values, the total color change was determined using the equation (1). The detailed descriptions of the method can be found elsewhere.[26, 27]

$$\Delta E^* = \sqrt{(\Delta L^*)^2 + (\Delta a^*)^2 + (\Delta b^*)^2} \quad (1)$$

where ΔL*, Δa* and Δb* are the difference between the coated and the uncoated (control) samples.

3.6 Attenuated total reflection- infrared (ATR-IR) spectroscopy. A Bruker Alpha ATR-FTIR spectrometer at a scan range of 4000-650 cm^{-1} was used to analyze the chemical composition of the coated and uncoated papers. A total of 32 scans were performed with a resolution of 4 cm^{-1}.

3.7 Static Contact angle (SCA) measurements. The water wettability of coated and uncoated papers were measured by using a OCA15+ contact angle measurement system (Dataphysics, Germany) with the sessile drop method and a drop volume of 3 µl. All measurements were carried out at room temperature. Determination of the SCA was based on the analysis of the drop shape by the Young-Laplace method and was performed with the software provided by the manufacturer (software version SCA 20). All the measurements were performed on at least three independent substrates with a minimum of ten drops per surface and an average value was calculated.

3.8 Alkaline reserve and pH determination. The alkaline reserve (AR) (meq(OH^-)/100 g paper) was determined by back-titration according to the standard method ASTM D4988-96R01. Briefly, papers (1 g) were cut into 5 x 5 mm^2 and placed it in Erlenmeyer flask (125 mL) containing 25 mL of MQ-water and 20 mL of 0.1 M HCl. The mixtures were heated to boiling. After boiling it for 1 min it was cooled down to room temperature. Following this three drops of methyl red indicator were added. The mixtures were then titrated with 0.1 M

NaOH up to the end point (color change from red to first lemon-yellow). The alkaline reserve was determined using the equation (2-3)

$$\text{Alkalinity as } Mg(OH)_2 = \frac{[(V_{HCl} \text{ x } N_{HCl}) - (V_{NaOH} \text{ x } N_{NaOH})] \text{ x } 0.029 \text{ x } 100}{DW} \quad (2)$$

where 0.029 is the milliequivalent weight of $Mg(OH)_2$ and DW is the dry weight of the specimen (in g).

Alkaline reserve (meq $[OH^-]$/100 g paper mass)

$$= \frac{[(V_{HCl} \text{ x } N_{HCl}) - (V_{NaOH} \text{ x } N_{NaOH})]}{\text{Dry weight of paper (g)}} \text{ x } 100 \quad (3)$$

The cold-extract pH of the papers was determined according to the standard method TAPPI T509 om-88, scaled down to 0.5 g of paper. Briefly, papers (0.5 g) were cut into 5 x 5 mm^2 and placed it in 50 mL beaker. Then, 5 mL of MQ-water was added and the mixtures were macerated with a flattened glass stirring rod until the papers were wet. Afterwards, 30 mL of MilliQ-water was added, stirred for 1 h, covered with a watch glass covered, allowed to stand for few minutes at room temperature, and the pH was measured. All the experiments were carried out at least three times.

For determination of pH and alkaline reserve for peeled samples, at least 1 g of paper were collected (from the peeling experiments as mentioned in section 2.3) and cut into 5 x 5 mm^2. Several coated paper sheets (4 x 5 cm^2) were used for peeling to obtain at least 1 g of material.

3.9 Mechanical properties. The tensile strength at maximum (MPa) and the tensile strain at break (%) of the papers were measured according to the standard method TAPPI T494 om-01 using a Shimadzu AGS-X electromechanical universal testing machine.[28] For testing, the papers were cut into a size of 4 mm x 5 cm and vertically mounted with two clamps with 2.5 cm distance between the clamps. Papers were tested at a speed of 1 mm min^{-1} with a 5 kN

load cell. At least ten experimental runs were carried out and average values and standard deviations were calculated. All papers were conditioned at 23ºC and 65% RH for 24 h before the test.

4. RESULTS AND DISCUSSION

4.1 Kinetic stability, particle size and morphology of unmodified and TMSC stabilized $Mg(OH)_2$ NPs

For many applications, an important goal is to enhance the stability of nanoparticle dispersions during transportation storage and use. One common strategy to control the aggregation of nanoparticles in solution is to add polymers, which act as a steric stabilizer preventing uncontrolled aggregation.[29, 30] At present synthetic polymers are employed more frequently.[29, 31] In our case, we have chosen TMSC as a stabilizer since polysaccharides in general are biocompatible and beneficial for paper conservation. The kinetic stability of the nanoparticles in solution can be easily examined by UV-Vis spectroscopy. Figure 1 shows the UV-Vis absorbance (600 nm) of $Mg(OH)_2$ (1%, w/v) dispersed in HMDSO with and without TMSC as a stabilizer (0.1, 0.5 and 2%, w/v). Pure $Mg(OH)_2$ NPs dispersed in HMDSO settles down rapidly within the first minutes as indicated by a sudden drop in absorbance (Figure 1, a). In contrast, $Mg(OH)_2$ NPs stabilized with TMSC shows a much higher stability (absorbance above 80%) (Figure 1 b-d). This is further shown by the photographs in Figure 1 (insert). The pure $Mg(OH)_2$ NPs dispersed in HMDSO solvent completely sediment while TMSC (2%, w/v) stabilized $Mg(OH)_2$ NPs remained as a stable colloidal dispersion. Obviously, with an increase in TMSC concentration the particle dispersibility and colloidal stability is increased, indicating an enhanced interaction between the particles and the polymer. TMSC offers steric repulsion and hydrophobization of nanoparticles due to its high molecular weight and its trimethylsilyl (TMS) groups which prevent the particles from

uncontrolled aggregation. Although a slight and constant decrease in absorbance is noticeable for particles stabilized with lower TMSC concentration (0.1-0.5%, w/v), the absorbance is nearly constant at a high TMSC concentration (2%, w/v) throughout the whole duration of the test. It should be noted that the 3 h time-span of the test is considered sufficient for practical applications. For further analysis and deacidification, dispersions containing 1 % (w/v) $Mg(OH)_2$ and 2 % (w/v) TMSC are employed since they show high colloidal stability and contain sufficient amounts of alkaline particles.

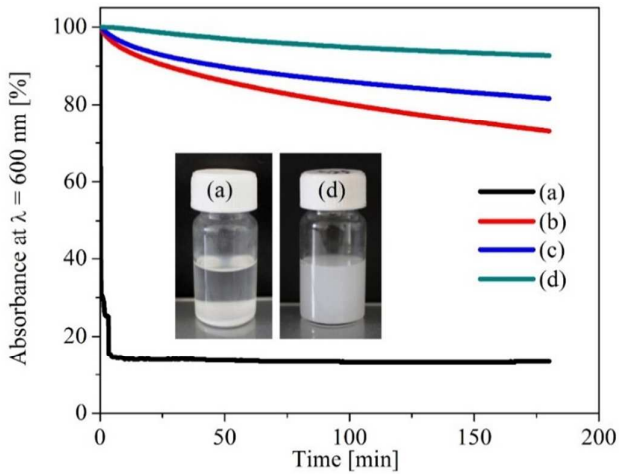

Figure 1. Absorbance of $Mg(OH)_2$ NPs dispersed in HMDSO (a) and in TMSC (b: 0.1 % w/v, c: 0.5 % w/v, d: 2 % w/v) at 600 nm wavelength.

The mean particle size of $Mg(OH)_2$ NPs (1%, w/v) dispersed in HMDSO and in TMSC solution (2%, w/v), measured by DLS, were found to be 838 ± 15 and 150 ± 3 nm. Besides that, TEM analysis was performed to determine the particles size in dry condition and compared it with the results from DLS measurements. TEM images of $Mg(OH)_2$ NPs (1%, w/v) dispersed in HMDSO and in TMSC solution (2 %, w/v), and their corresponding particle size distributions in the dry state are shown in Figure 2. As expected, $Mg(OH)_2$ NPs dispersed in polymer free HMDSO shows a clear agglomeration of spherical-shaped particles with

average diameter of 46 ± 2 nm (a-b). In the presence of TMSC an agglomeration of NPs is still visible and the spherical morphology is less pronounced (c). Interestingly, the size of the single particles remain unchanged (45 ± 3 nm, d) after hydrophobisation with TMSC. Obviously the particles measured by TEM are much smaller than the mean particle size measured by DLS. The latter measure the mean hydrodynamic diameter, whereas TEM give the single and vacuum dried particles. It is well-known that the hydrodynamic size of the particles which are dispersed in liquids are usually larger than the primary particle size *i.e.* single particle, as reported in many other studies.[32-34] From that viewpoint, we can propose that during DLS analysis, an agglomerate of many single particles ($Mg(OH)_2$ or TMSC-$Mg(OH)_2$ NPs) are measured as one large particles. However, during TEM analysis the average particle size of the individual particles that form an agglomerate is determined.

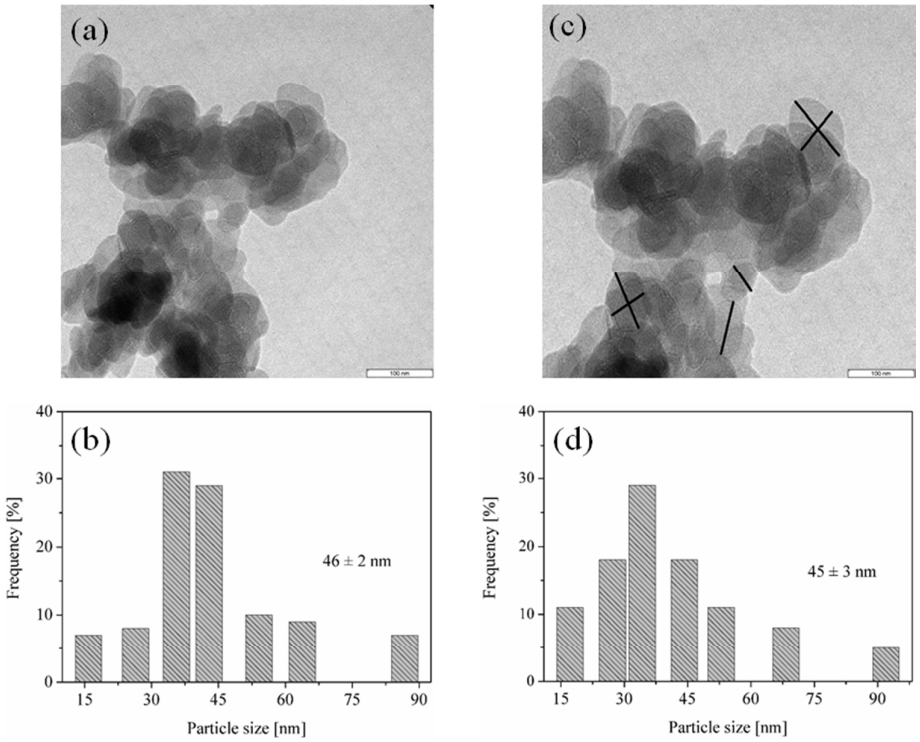

Figure 2. TEM images (top) and particle size distribution (bottom) of $Mg(OH)_2$ NPs dispersed in HMDSO (a,b) and in HMDSO/TMSC (2 %, w/v) (c,d).

4.2 Optical appearance of coated and aged papers

Accelerated aging is one of the primary interests in library and archival preservation science in order to determine the long term effect of conservation treatment and the life span of the paper coated with the deacidifying components. Such tests are usually performed at elevated temperature and constant relative humidity. In our study, we conducted the accelerated aging test at 80°C and at 75 % RH for both filter and HWP papers. Filter paper is used as a quasi-standard in research and in the paper conservation and restoration. Moreover, filter paper is chemically and structurally somehow similar to HWP paper, and is nearly included as a standard testing material in the evaluation of all new deacidification methods therefore. Due to the above mentioned properties, filter papers are chosen as a reference paper although it does not contain any sizing components, in our case, for analysis of the degradation of cellulose after the deacidification and artificial aging.

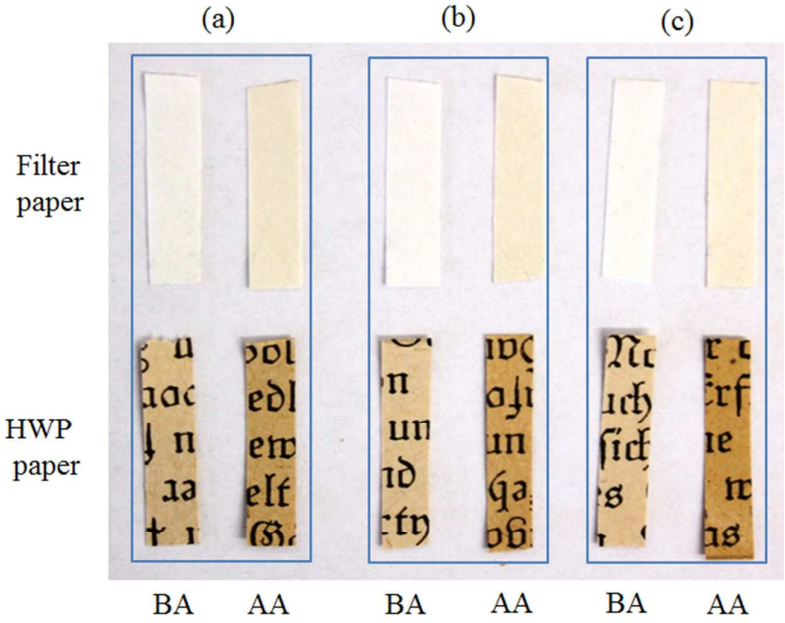

Figure 3. Uncoated and treated paper sheets before and after artificial aging. (a) Uncoated papers, (b) papers coated with TMSC and (c) papers coated with TMSC-$Mg(OH)_2$ NPs. BA – before aging and AA- after aging.

The macroscopic images of the uncoated and coated filter and HWP papers before and after artificial aging are shown in Figure 3. It is obvious that coating with either TMSC or TMSC stabilized $Mg(OH)_2$ NPs (and/or aggregates) does not cause visible deposits or other changes in the dimensions or appearance of the uncoated papers. This is further supported by the finding from the color measurements (see section 4.3). However, a color change *i.e.* yellowing occurs already on the uncoated papers due to aging. This effect is also visible on papers that are coated with TMSC and TMSC-$Mg(OH)_2$ NPs. As mentioned above, an important reaction during aging is the hydrolytic degradation of cellulose macromolecules due to acidity in paper. The yellowing of paper upon aging can be attributed to the presence of chromosphores formed from the degradation of one or more components (like cellulose, lignin and hemicellulose).[35] However the oxidation of cellulose cannot be avoided during an accelerated aging (at temperature of 80°C and at 75 % RH), leading to an increased acidity followed by yellowing in paper. Upon aging the papers coated with mixtures of TMSC/deacidifying components are turned into more yellow in color compared to uncoated and aged papers. Even though this can be seen as one drawback of our method, the additional yellowing can be prevented or avoided by controlling the final pH of the paper by coating with a lower particles concentration (see section 4.3 and 4.7).

4.3. Colorimetric measurements

To verify the discoloration of uncoated and coated papers (before and after aging) the colorimetric measurements were performed. The results of the CIE color coordinates (L, a,

b)* are presented in Table 1. The results showed that the discoloration (*i.e.* yellowing) occurred already on uncoated and aged papers. Obviously, filter paper showed more yellowing (ΔE* = 13.4) than that of HWP one (ΔE* = 10.3), indicating that uncoated filter paper undergoes a fast degradation and more susceptible to oxidation. After coating with TMSC and aged no significant changes in yellowing is observed. However, the yellowing is increased up to 4 % (ΔE* = 14.1) and 18 % (ΔE* = 12.5) for filter and HWP paper compared to uncoated and aged papers. The increased yellowing for HWP paper maybe due to the high pH (9) obtained by TMSC-$Mg(OH)_2$ NPs coating (Table 5 and S1, see ESI). As reported by other authors, a pH value of above 9 can be dangerous for oxidized papers, leading to more degradation, and consequently to more yellowing.[2] To verify this HWP paper (coated 0.25 % (w/v) particles concentration) that showed a value close to neutral pH (7.6 ± 0.3, see section 4.7) was chosen and subjected to artificial aging as mentioned above. The results showed that the yellowing (ΔE* = 10 ± 0.1) remained unchanged compared to uncoated and aged paper (ΔE* = 10.3 ± 0.1), while it decreased to 28% compared to HWP paper (Table S1-S2, see ESI) which is coated with higher particles concentration (1%, w/v) and had a pH value of 9 (see Table 5). Similar results are obtained for filter paper whose pH was 7.5 ± 0.1 after coating with 0.0625% (w/v) particles concentration. These results confirm that the yellowing can be avoided for deacidified papers having neutral pH upon aging. Moreover, it can be noticed that the brightness (L*) value is not changed for coated and non-aged papers, confirming that the color of the papers is retained after the application of our coating. In general, the yellowing is caused by the formation of chromophore, which is the results of degradation of one or more components present in HWP paper as mentioned before.

Table 1. CIE color coordinates of uncoated and coated papers

Samples	Filter paper				HWP paper			
	L	a*	b*	ΔE*	L	a*	b*	ΔE*
Uncoated	96.3	0.02	3.7	0.0	82.1	3.0	15.8	0.0
Uncoated, aged	88.9	3.0	14.6	13.4	73.4	5.7	20.4	10.3
TMSC coated	96.3	0.01	3.9	0.0	82.3	3.1	17.1	0.0
TMSC coated, aged	87.6	2.7	13.1	13.0	73.4	6.1	21.1	10.2
TMSC-$Mg(OH)_2$ coated	96.3	0.02	4.0	0.0	82.1	3.0	18.0	0.0
TMSC-$Mg(OH)_2$ coated, aged	86.3	2.5	13.5	14.1	70.7	5.0	22.8	12.5

4.4 Microscopic morphology of the coatings

The SEM images of the uncoated filter and HWP paper are depicted in Figure 4a. It can be seen that both materials have the common fibrillar microstructure. A certain smoothening effect of the fiber surface can be observed after TMSC coating (b). The images of TMSC coated papers after aging are shown in the supporting information (ESI, Figure S1) and showed clumps of aggregates deposited on the fiber surfaces of HWP paper at least compared to the non-aged samples. By treating filter and HWP paper with the TMSC stabilized nanoparticle dispersions homogeneous particle deposits are immobilized on the fiber surfaces (c). Almost full coverage of a thin particle layer is obtained. The thickness of this layer is of importance since transparency of the coatings is necessary and no white deposits are visible. After aging for two weeks at 80°C, no morphological changes of the particle coatings are observed and $Mg(OH)_2$ is retained on the surface (d).

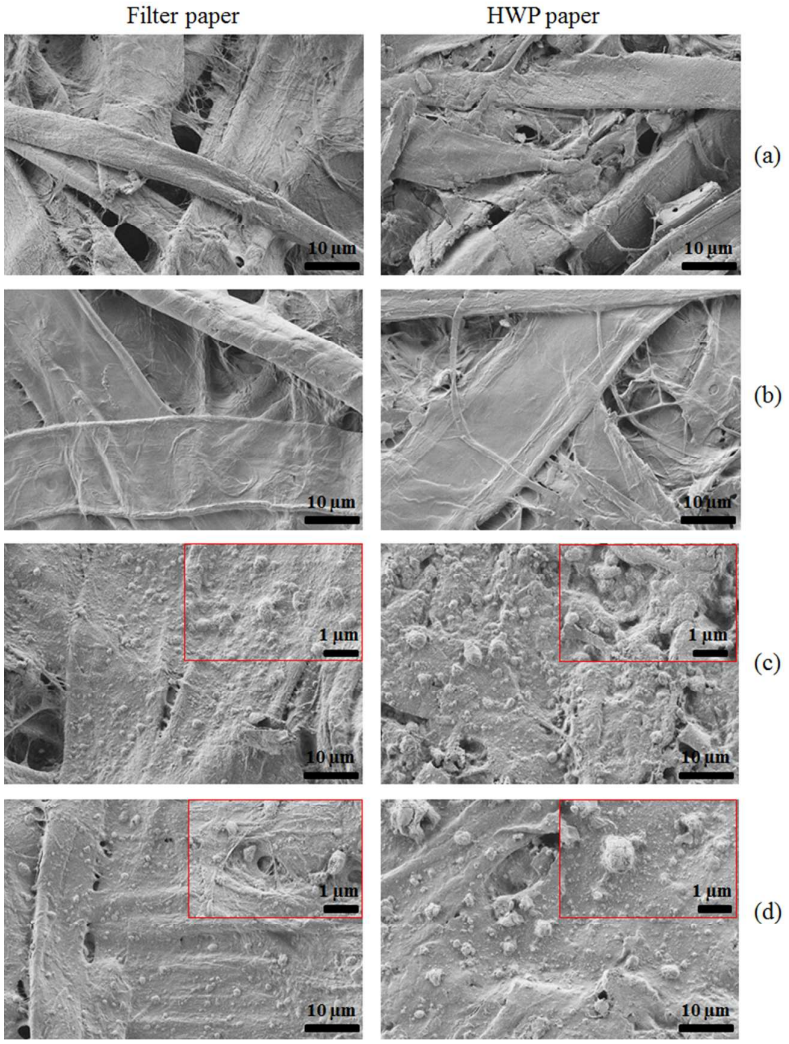

Figure 4. SEM micrographs of (a) uncoated paper, (b) TMSC coated before aging, (c) TMSC-$Mg(OH)_2$ coated before aging, (d) TMSC-$Mg(OH)_2$ NPs coated after aging.

To verify the deposition or distribution of particles at the inner surfaces of paper the coated materials from the top few layers of paper were peeled off using an adhesive tape (see section 2.3) and the samples that remained after peeling were analyzed by SEM. The SEM micrographs of uncoated and coated papers after peeling-off one and five times are shown in Figure 5. It can be seen that the fibrillar structures of peeled samples are changed (a-b)

comparing to the original ones (Figure 4a, right). For coated papers whose surfaces were peeled-off once, smaller and larger agglomerated nanoparticles are visible as indicated by the arrows (c). Interestingly, this is also noticeable on surfaces that were peeled-off five times (d). This is further supported by EDX elemental mapping (Figure S3-S4, see ESI), which clearly shows the presence of magnesium and silicon (as indicated by the bright spots) in one time peeled as well as in five times peeled samples similar to unpeeled coated samples (Figure S2, see ESI), but to a lesser extent. The results suggest that the functionalized alkaline particles are small enough to penetrate/diffuse through the pores of paper in the liquid environment. The penetration of the nanoparticles into the core of the paper is also verified by water contact angle measurements see section 4.6. Further it can be concluded that the method allows to deposit alkaline components inside the paper by a simple diffusion process, which is necessary to ensure a complete neutralization of acidity and a longer prevalence of treatment.

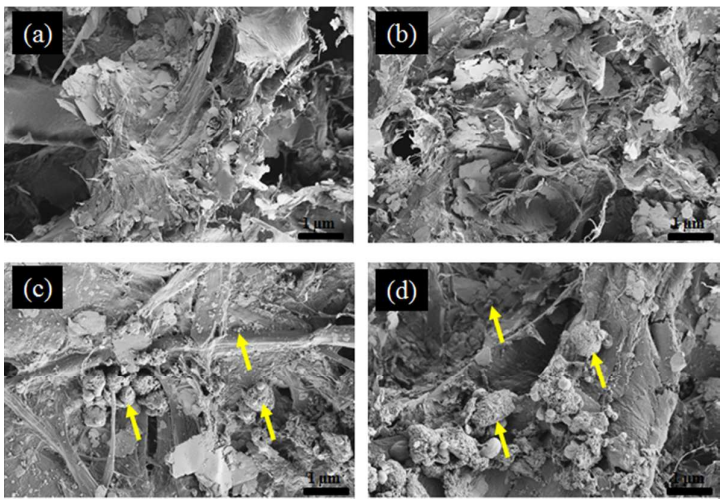

Figure 5. SEM micrographs of uncoated (top) and TMSC-$Mg(OH)_2$ NPs coated (bottom) HWP paper. Once peeled (a, c), and five times peeled (b, d).

The layer thickness and the mass loss of the peeled samples were also measured and the results are presented in Table 2. As expected, both filter and HWP paper showed a reduced layer thickness and mass as a result of peeling. For filter paper the thickness and the mass are decreased to 14 and 33.5% after one time peeling. While the HWP paper showed a 14% reduction in film thickness similar to filter paper, the mass is decreased to 20.5%. Whereas, five times peeling resulted in 36 and 29% reduction in layer thickness for filter and HWP paper, and the mass loss is close to 40% for both papers.

Table 2. The film thickness and mass loss of the TMSC-$Mg(OH)_2$ NPs coated and uncoated papers before aging.

Peel	Filter paper		HWP paper	
	Thickness (μm)	Mass t loss (%)	Thickness (μm)	Mass loss (%)
0	140 ± 2	-	140 ± 2	-
1	120 ± 10	34	120 ± 2	33
5	90 ± 10	39	100 ± 10	38

Table 3 shows the amount of magnesium and silicon present in the uncoated and coated papers before and after aging, obtained from EDX analysis (in at.%). While no silicon is detected on uncoated filter and HWP paper, the papers coated with TMSC show the presence of silicon (filter paper: 2.9 ± 0.2 at.%, HWP paper: 4.8 ± 0.5 at.%) confirming that the papers are successfully coated with TMSC. Interestingly the HWP paper shows higher amounts of deposited TMSC. A plausible reason can be that the old HWP paper contains more pores and exhibits a higher surface roughness, allowing the uptake of more TMSC. An enhanced TMSC deposition is noticed (filter paper: 7.9 ±0.3 at.%, HWP paper: 11.2 ± 0.3, at.%) when dispersion containing $Mg(OH)_2$ NPs are employed. In this case, it can be assumed that $Mg(OH)_2$ NPs with a larger surface area facilitates the incorporation of higher amounts of TMSC. The papers that are coated with TMSC and subjected to accelerated aging show no

silicon, demonstrating that the coated TMSC is hydrolyzed into cellulose. Higher humidity and temperature can hydrolyze TMSC into cellulose by cleaving of O-Si bonds from the TMSC backbone. Upon aging TMSC will be converted into corresponding silanol, which undergoes condensation reaction to give hexamethyldisiloxane (HMDSO). The later compound with low surface tension is rather volatile can and be removed from the surface as soon it is formed.[20] In contrast for papers coated with TMSC-$Mg(OH)_2$ NPs no significant reduction in silicon is noted after aging. This implies that the presence of $Mg(OH)_2$ essentially prevents complete hydrolysis of TMSC, most likely due to sterical hindrance and reduced accessibility for water. The filter and HWP paper coated with TMSC-$Mg(OH)_2$ NPs shows 8 and 22% reduction in magnesium after aging, indicating that some $Mg(OH)_2$ is converted into the carbonate form by reacting with carbon-di-oxide (CO_2) or into its corresponding $MgSO_4$ salt upon neutralization with acids.[23] It has to be noted that distribution of atomic ratio of magnesium is less in $MgCO_3$ or in $MgSO_4$ compared to $Mg(OH)_2$. Therefore, a lower magnesium content is detected by EDX for papers coated with TMSC-$Mg(OH)_2$ NPs after aging.

Table 3. Magnesium and silicon content of uncoated and coated papers, obtained from EDX analysis. The values were obtained from the average of six independent measurements from two samples. For clarity reasons the values of other elements are given in the supporting information (Table S3-S4).

	Filter paper		HWP paper	
	Mg (at. %)	Si (at. %)	Mg (at. %)	Si (at. %)
Uncoated	n.d	n.d	n.d	n.d
TMSC coated (before aging)	n.d	2.9 ± 0.2	n.d	4.8 ± 0.5
TMSC coated (after aging)	n.d	n.d	n.d	n.d
TMSC-$Mg(OH)_2$ NPs coated (before aging)	11.8 ± 0.4	7.9 ±0.3	23.2 ± 1.0	11.2 ± 0.3
TMSC-$Mg(OH)_2$ NPs coated (after aging)	10.8 ± 0.5	6.5 ± 1.0	18.2 ±1.0	10.8 ±0.9

4.5 Attenuated total reflection infrared spectroscopy (ATR-IR) analysis

The ATR-IR spectra of filter and HWP paper of the different coatings are shown in Figure 6. Compared to uncoated paper (a), peaks for the C-Si rocking vibrations (at 757, 1250 and 840 cm^{-1}) are observed for papers coated with TMSC and TMSC-$Mg(OH)_2$ NPs (b and c). In addition the peaks corresponding to O-H stretching vibrations of $Mg(OH)_2$ NPs are detectable at 3695 cm^{-1} (c). Interestingly, the C-Si peaks disappeared completely for papers coated with TMSC (without $Mg(OH)_2$ NPs) after aging (Figure S5, see ESI), confirming that during aging TMSC is hydrolyzed into cellulose, by cleavage of the O-Si bond from the TMSC backbone.[19-21] This data supports the finding from the EDX analysis that also showed no detection of silicon for aged TMSC coated paper samples. In contrast the C-Si bonds are still present in TMSC-$Mg(OH)_2$ NPs coated paper (d). The presence of a dense $Mg(OH)_2$ layer obviously protects the TMSC to be hydrolyzed during aging. Again, the latter results correlate

very well with the EDX analysis where no major reduction in silicon content is observed for the TMSC-$Mg(OH)_2$ NPs coated paper after aging (see Table 3). The results also showed no additional peaks, before and after aging, for the formation of carbonate ion (CO_3^{2-}), implying that no conversion is taken place from $Mg(OH)_2$ to magnesium carbonate ($MgCO_3$). A likely explanation is that the protective TMSC layer may inhibit the carbonate formation or the concentration of $MgCO_3$ is too low to be detected (if it is formed), creating a less safe environment compared to the one which could be generated by $MgCO_3$.

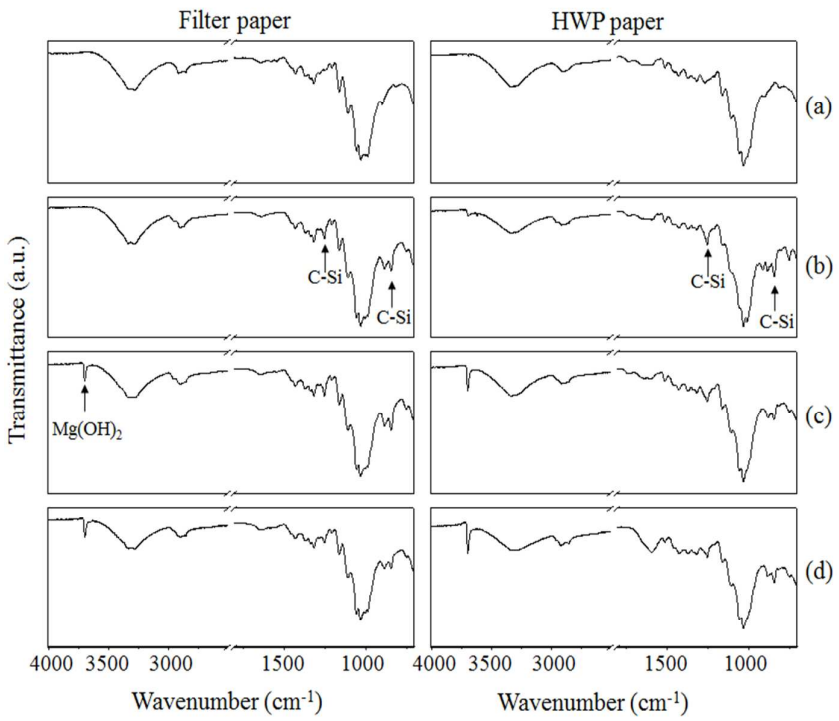

Figure 6. ATR-IR spectra of uncoated and coated paper before and after aging. (a) uncoated paper, (b) TMSC coated before aging, (c) TMSC-$Mg(OH)_2$ NPs coated before aging (d) TMSC-$Mg(OH)_2$ NPs coated after aging.

4.6 Contact angle measurements

The wettability of paper coated with TMSC and TMSC-$Mg(OH)_2$ NPs before and after aging was determined by water contact angle measurements (Table 4). Uncoated filter paper is obviously completely wetted. In contrast, uncoated HWP paper is highly hydrophobic (CA)H_2O: 125°. This can be attributed to the presence of different components in paper, such as lignin and sizing agents[36], and a generally low moisture content. After coating with TMSC, a high (CA)H_2O:125° is noticed for both papers confirming the successful deposition of TMSC on filter paper and supporting the findings from the EDX analysis and ATR-IR measurements. Higher (CA)H_2O values are well-known for TMSC coated surfaces as reported elsewhere.[37, 38] As mentioned above, aging results in the cleavage of O-Si bonds and leads to cellulose formation with higher water wettability.[19, 39] Upon aging the surface of TMSC coated filter paper becomes again completely hydrophilic ((CA)H_2O not measurable) and HWP paper treated in the same way also has a much lower ((CA)H_2O confirming the hydrolysis of TMSC. Filter paper coated with TMSC-$Mg(OH)_2$ NPs shows similar (CA)H_2O as pure TMSC coatings confirming the presence of polymer and particles. After aging contact angles are not decreased on these coatings. These results are comparable with the data derived from IR measurements where the C-Si peaks are still present on the aged paper. Retaining the hydrophobicity even after aging would be advantageous for paper conservation since a hydrophobic paper surface could reduce the uptake of moisture from the surrounding environment. However the formation of cellulose during aging does also not impose any risk on paper and can be seen advantageous in terms of the materials` compatibility.

Table 4. Water contact angles of coated and uncoated papers before and after aging.

	Filter paper	HWP paper
Uncoated	Not measurable	126 ± 2
Uncoated, aged	Not measurable	123 ± 3
TMSC coated	124 ± 4	128 ± 3
TMSC coated, aged	Not measurable	92 ± 5
TMSC-$Mg(OH)_2$ NPs coated	133 ± 3	126 ± 3
TMSC-$Mg(OH)_2$ NPs coated, aged	140 ± 3	122 ± 3

As mentioned in section 4.4, contact angles measurements were performed to confirm the penetration of TMSC-$Mg(OH)_2$ NPs into the inner structure of the peeled samples. For this purpose, the (CA)H_2O are measured for both filter and HWP paper (uncoated and coated) that were peeled for five times. As expected no differences in (CA)H_2O for peeled coated (142 ± 5°) and uncoated (142 ± 5°) HWP paper is observed. This is due to the fact that HWP paper contains different hydrophobic sizing components giving no changes in the contact angle values. Whereas, peeled uncoated filter paper, which contains 100% pure cellulose and no sizing components, yielded (CA)H_2O:0° (like in the case of unpeeled sample). In contrast (CA)H_2O of 130 ± 7° is obtained for coated and peeled sample giving a solid evidence that the hydrophobic TMSC-Mg(OH) NPs are penetrated into inner fiber structure of the paper.

4.7 Alkaline reserve (AR) and pH determination

The neutralization of acids and the introduction of an alkaline reserve (AR) in paper is highly important in paper conservation to prevent or slow down further hydrolysis. The pH and alkaline reserve of coated and uncoated filter and HWP paper before and after aging are given in Table 5. As expected, uncoated filter paper exhibits a pH of 7 and no alkaline reserve. Interestingly the pH of TMSC coated papers (both filter and HWP) is increased by one unit,

suggesting that TMSC coating also contributed to the pH increase. This is confirmed by measuring the pH of TMSC dispersed in pure MilliQ-water where a pH value of 8 ± 0.3 is obtained compared to the pH (7 ± 0.1) of MilliQ-water without TMSC. After treatment with TMSC-$Mg(OH)_2$ NPs, a pH of 10 and an alkaline reserve (AR) of 47 meq [OH^-]/100 g is reached. The AR in this case is corresponds to 1.4 wt.% of $Mg(OH)_2$. Interestingly after aging no large change in pH and alkaline reserve are noticed. These data fits very well to the results obtained from the EDX analysis where almost no major reduction in magnesium is noticed for paper coated with TMSC/$Mg(OH)_2$ mixture after aging. However, uncoated HWP paper is acidic with a pH of 4 as determined by pH measurement. Similar to filter paper, coating with TMSC did not result in any changes of alkaline reserve. By treatments of HWP paper with TMSC/$Mg(OH)_2$ NPs mixture, the pH and the alkaline reserve are increased to 9 and 61 meq [OH^-]/100 g (corresponding to 1.8 wt.% $Mg(OH)_2$). Although pH 9 can be considered as an 'unsafe' value for oxidized HWP paper that requires deacidification and an additional alkaline reserve as stated by other authors[2], the pH of the final coated paper can easily be tuned depending on the chosen nanoparticles concentration (see below). After aging the pH and the alkaline reserve are significantly decreased to 8 and 41 meq [OH^-]/100 g (*i.e.*1.2 wt.% $Mg(OH)_2$) confirming the consumption of some $Mg(OH)_2$ by neutralization reactions with acids present in HWP paper. As mentioned above, acid neutralization with $Mg(OH)_2$ can possibly leads to the formation of its corresponding salt such as magnesium sulfate ($MgSO_4$), which does not contributes to the alkaline reserve, and therefore a less alkaline reserve is determined. As shown in Table 5 the pH of uncoated filter paper is 7 and it does not need deacidification. Therefore no alkaline reserve is consumed upon aging. By using TMSC/$Mg(OH)_2$ NPs mixture it is possible to eliminate the acidity and to simultaneously introduce a sustainable alkaline reserve to paper by a very simple but efficient process.

Table 5. Alkaline reserve (AR in meq[OH^-]/100g of paper)) and pH of coated and uncoated paper before and after aging.

Samples	Filter paper			HWP paper		
	pH	AR	$Mg(OH)_2$ (wt.%)	pH	AR	$Mg(OH)_2$ (wt.%)
Uncoated	7 ± 0.1	-	-	4 ± 0	-	-
Uncoated, aged	7 ± 0.3	-	-	4 ± 0	-	-
TMSC coated	8 ± 0.3	-	-	5 ± 0.2	-	-
TMSC coated, aged	8 ± 0.1	-	-	5 ± 0.1	-	-
TMSC-$Mg(OH)_2$ coated	10 ± 0.1	47 ± 1	1.4	9 ± 0.3	61 ± 6	1.8
TMSC-$Mg(OH)_2$ coated, aged	10 ± 0.1	47 ± 2	1.4	8 ± 0.1	41 ± 2	1.2

To determine the amount of alkaline reserve (AR) deposited inside the paper sheets the coated materials from the front and back side of the paper were peeled-off, and the samples that remained after peeling were analyzed by back-titration. In addition the pH was measured and compared with results of the alkaline reserve (Table 6). Surprisingly an increase of 14 wt.% $Mg(OH)_2$ deposition (AR: 54 meq[OH^-]/100g) and almost no change in pH are observed for filter paper after peeling one time compared to unpeeled samples, confirming that more material is deposited or diffused into the porous fiber structure of paper. Even though the thickness is reduced 36% after five times peeling as mentioned above, no significant changes in alkaline reserve and pH are observed. This is an evidence that the nanoparticles are equally deposited/distributed in the entire inner paper surface. However, a different behavior is observed in the case of HWP papers. After first peeling the alkaline reserve is decreased to 50% (31 meq[OH^-]/100g) and remained almost constant after five times, but no major changes in pH are observed similar to filter paper. Over all, our coating provided an approx. 2 wt.% $Mg(OH)_2$ (55 meq[OH^-]/100g) and pH of 11 for filter paper, and approx. 1 wt.%

$Mg(OH)_2$ (29 meq[OH^-]/100g) and pH of 8 in the case of HWP paper even after five times peeling. From the above results it can be confirmed that our treatment is highly efficient, and enabled the irreversible deposition of alkaline nanoparticles not only on the surface but also at the inner paper fiber structure, which is highly important for further neutralizing the acids that can be generated during storage and preservation.

Table 6. Alkaline reserve (AR in meq[OH^-]/100g of paper)) and pH of TMSC-$Mg(OH)_2$ NPs coated HWP paper before and after peeling.

Peel	Filter paper			HWP paper		
	AR	$Mg(OH)_2$ wt.%	pH	AR	$Mg(OH)_2$ wt.%	pH
0	47 ± 1	1.4	10 ± 0.1	61 ± 6	1.8	9 ± 0.3
1	54 ± 3	1.6	11 ± 0.1	31 ± 5	0.9	8 ± 0.2
5	55 ± 9	1.6	11 ± 0.1	29 ± 1	0.8	8 ± 0.1

Papers were also coated with lower concentrations of TMSC-$Mg(OH)_2$ NPs as shown in section 2.3 in order to tune the final pH of the coated papers. At the concentration of 0.0625% (w/v) a pH of 7.5 ± 0.1 and an alkaline reserve of 3.8 ± 0.1 meq [OH^-]/100 g (corresponding to to 0.1 % wt.% $Mg(OH)_2$) are obtained for filter paper. Whereas in the case of HWP paper the pH of 7.6 ± 0.3 and the alkaline reserve of 9.1 ± 0.3 meq [OH^-]/100 g (corresponding to 0.3 % wt.% $Mg(OH)_2$) are reached with 8-fold higher particles concentration (0.25 % (w/v)). Obviously after the deacidification a neutral pH is obtained creating a safer environment for the papers. After aging the samples for two weeks the changes in pH and alkaline reserve are almost negligible for filter paper, while the decrease in pH and alkaline reserve are one unit and 22 % for HWP paper (Table S5, see ESI), respectively. The outcome from these measurements is in line with the results obtained with higher particles concentration where a similar reduction in pH and alkaline reserve are noted upon aging.

An important issue in the paper conservation is to bring a 'safer' pH value (*i.e.* between 6.5-7.5) after the deacidification.[9] In this context, several non-aqueous methods have been

proposed to meet the above demand. For example in the recently established method by Poggi et al. an alcoholic dispersions of $Mg(OH)_2$ NPs are employed to reach the final pH of ca.7 for the deacidified paper, with a single treatment.[9] Likewise, a dispersion of magnesium oxide (MgO) in non-polar fluorinated surfactant is used in the 'Bookkeeper' method, which allows to tune the final pH of the treated paper between 7 and 10.[40] Wei T'O is another well-known method, which uses magnesium-methoxy methyl carbonate (MMC) solutions in ethyl or methyl alcohol and chlrofluorocarbons (CFC).[41] Upon contact with water from the paper or from the surrounding atmosphere MMC is hydrolysed into reactive $Mg(OH)_2$, leading to acid neutralization and formation of protective magnesium carbonate ($MgCO_3$) layer. This method also gives the possibility to alter the pH values of the deacidified papers from 7.5 to 10.4. It is obvious that the final pH of the treated paper can be easily tuned from neutral to high pH (10) by the above mentioned methods. These results, in general, are comparable with the pH values (between 7.6 and 9 depending on the chosen particles concentration) obtained by our treatment that employed also $Mg(OH)_2$ NPs, which are stabilized in TMSC/HMDSO. The different deacidification methods described above are very efficient in acid neutralization and providing additional alkaline reserve that prevents papers from further degradation. However, nanoparticles of $Mg(OH)_2$ stabilized in TMSC/HMDSO or alcohol offer certain advantages than the above mentioned methods and do not give the possible drawbacks owing to the use of fluorinated surfactants or fluorocarbons for the stabilization of deacidifying agents. Moreover, the long-term effect of fluorinated surfactants or hydrocarbons that is present on the paper after the deacidification have not been investigated in detail until now.

4.8 Mechanical strength determination

In addition to the introduction of an alkaline reserve and the neutralization of acids, strengthening of old and brittle paper is of high interest. Therefore, we investigated the role of

TMSC in the improvement of mechanical properties such as tensile strength and tensile strain at break. The hypothesis would be that TMSC or cellulose formed out of it would result in an increased fiber-fiber bond and therefore higher tensile strengths. The mechanical properties of uncoated and treated filter and HWP paper are shown in Figure 7. A significant improvement in tensile strength and strain at break is obvious after coating with TMSC and TMSC/$Mg(OH)_2$. Upon TMSC coating, the increase in tensile strength at maximum for both filter and HWP paper is nearly 15 %. Mixtures of TMSC/$Mg(OH)_2$ resulted in a reduction of strength for filter paper whereas the strength of HWP paper coated with particles and polymer is similar to pure TMSC coatings. More significantly the tensile strain at break is increased up to 18 % for filter paper after TMSC coating and by 6 % for HWP paper. TMSC also increases the Young modulus of the paper (Table S6, see ESI), an indication that the paper becomes stiff. However, the application of TMSC-$Mg(OH)_2$ NPs decreased the stiffness *i.e.* increased elasticity, as shown by the reduced Young modulus. Imparting elasticity is highly beneficial in particular to HWP paper, which are rigid and brittle. In all cases, after aging a lower Young modulus is noted except for uncoated HWP paper. The TMSC/$Mg(OH)_2$ coatings lead to 74 % increase in the tensile strain at break for filter paper and 13 % increase for HWP paper, which is an indication that the compact mixture of particles and polymers on and in the fibers matrix have a profound impact on the mechanical properties. After aging, the tensile strengths of uncoated papers are decreased (14% for filter and 30 % for HWP paper), and also in the case of TMSC coated papers. TMSC/$Mg(OH)_2$ coated papers showed less reduction in strength (9 % for filter paper, 0.5 % for HWP paper). These results illustrate that treatment with TMSC/$Mg(OH)_2$ prevents further disintegration of paper upon aging and stabilizes the mechanical properties of paper. On the whole, it is an indication that the addition of TMSC and particles show a good compatibility with paper and improve the mechanical properties.

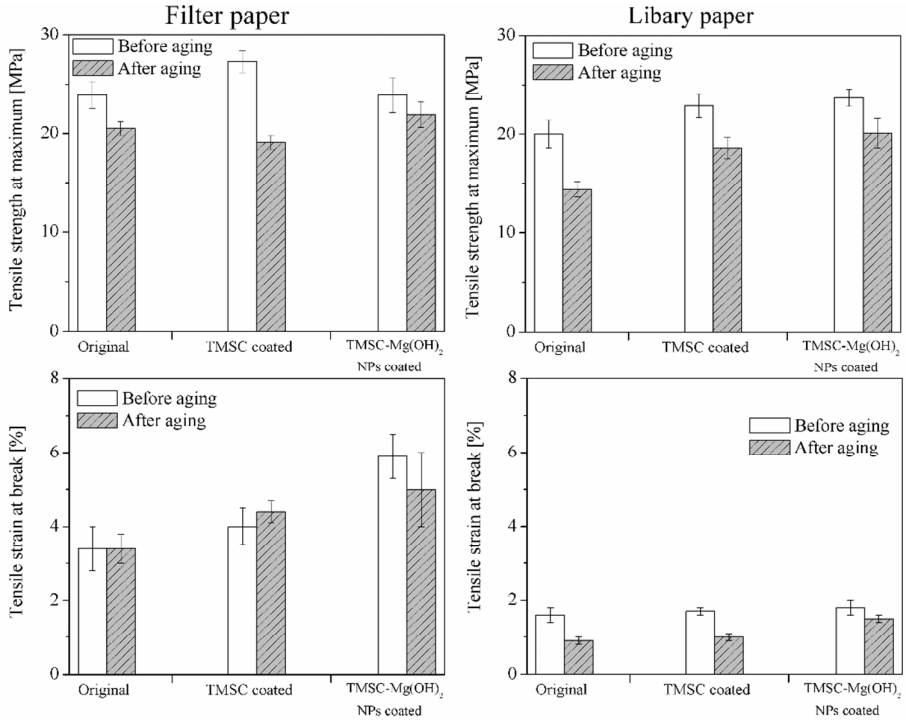

Figure 7. Tensile strength at maximum and tensile strain at break of coated and uncoated paper before and after aging.

5. CONCLUSIONS

We have demonstrated a simple and highly efficient deacidification method which simultaneously neutralizes acids, creates an alkaline reserve and improves the mechanical properties of filter and HWP paper. The application of trimethylsilyl cellulose (TMSC) strongly increases the colloidal stability of $Mg(OH)_2$ nanoparticles in the organic solvent hexamethyldisiloxane (HMDSO). Coating of these dispersions on papers results in thin, invisible hydrophobic alkaline layers that do not influence the appearance of non-aged and aged papers. The nano-coatings significantly increase the pH and alkaline reserve and result in higher tensile strengths before and after aging. Even though the effect of TMSC or TMSC-$Mg(OH)_2$ coating on the degree of polymerization of the papers before and after aging is not

analyzed in this work, this important parameter is essential to comprehend the degradation properties paper-based materials, which will be determined and published elsewhere. The method and treatment procedure is versatile and can be extended to other kinds of cellulose-based materials. As a final remark the nanoparticles coated with hydrophobic TMSC protective layer can be less dangerous, environmentally friendly and could reduce the health risk, which can be probably caused by usage of pure nanoparticles.

ACKNOWLEDGEMENT

The authors gratefully acknowledge financial supports from the Austrian Research Promotion Agency (FFG) and the Austrian Agency for International Cooperation in Education and Research (OeAD). Dr. Damien Faivre acknowledges funding from the European research council (Project MB2 °256915). Dr. Alenka Ojstrsek and Mojca Bozic from the University of Maribor, Slovenia are greatly acknowledged for their support regarding the colorimetric measurements.

REFERENCES

1. P. Baglioni, D. Chelazzi, R. Giorgi and G. Poggi, *Langmuir*, 2013, **29**, 5110-5122.
2. J. W. Baty, C. L. Maitland, W. Minter, M. A. Hubbe and S. K. Jordan-Mowery, *BioResources*, 2010, **5**, 1955-2023.
3. Z. Souguir, A.-L. Dupont, K. Fatyeyeva, G. Mortha, H. Cheradame, S. Ipert and B. Lavedrine, *RSC Advances*, 2012, **2**, 7470-7478.
4. D. Klemm, B. Heublein, H.-P. Fink and A. Bohn, *Angewandte Chemie International Edition*, 2005, **44**, 3358-3393.
5. R. Babu, K. O'Connor and R. Seeram, *Progress in Biomaterials*, 2013, **2**, 8.

6. D. Klemm, B. Philipp, T. Heinze, U. Heinze and W. Wagenknecht, *In comprehensive cellulose Chemsitry: fundamental and analytical methods*, Wiley-VCH, 1998.

7. M. Whitmore Paul and J. Bogaard, in *Restaurator*, 1994, vol. 15, p. 26.

8. X. Zou, N. Gurnagul, T. Uesaka and J. Bouchard, *Polymer Degradation and Stability*, 1994, **43**, 393-402.

9. G. Poggi, R. Giorgi, N. Toccafondi, V. Katzur and P. Baglioni, *Langmuir*, 2010, **26**, 19084-19090.

10. G. Poggi, N. Toccafondi, L. N. Melita, J. C. Knowles, L. Bozec, R. Giorgi and P. Baglioni, *Appl. Phys. A*, 2014, **114**, 685-693.

11. Z. Souguir, A.-L. Dupont, J.-B. d'Espinose de Lacaillerie, B. Lavédrine and H. Cheradame, *Biomacromolecules*, 2011, **12**, 2082-2091.

12. C. Piovesan, A.-L. Dupont, I. Fabre-Francke, O. Fichet, B. Lavédrine and H. Chéradame, *Cellulose*, 2014, **21**, 705-715.

13. E. Stefanis and C. Panayiotou, in *Restaurator*, 2010, vol. 31, p. 19.

14. L. Botti, O. Mantovani, A. Orrù Maria and D. Ruggiero, in *Restaurator*, 2006, vol. 27, p. 9.

15. E. Stefanis and C. Panayiotou, in *Restaurator*, 2008, vol. 29, p. 125.

16. Battelle-Institut, German patent No. DE 41 04 515 C1, 1992.

17. H. Cheradame, *Int Preserv News*, 2009, **48**, 5-8.

18. R. Kargl, T. Mohan, M. Bračič, M. Kulterer, A. Doliška, K. Stana-Kleinschek and V. Ribitsch, *Langmuir*, 2012, **28**, 11440-11447.

19. T. Mohan, R. Kargl, A. Doliška, A. Vesel, S. Köstler, V. Ribitsch and K. Stana-Kleinschek, *Journal of Colloid and Interface Science*, 2011, **358**, 604-610.

20. T. Mohan, S. Spirk, R. Kargl, A. Doliška, H. M. A. Ehmann, S. Köstler, V. Ribitsch and K. Stana-Kleinschek, *Colloids and Surfaces A: Physicochemical and Engineering Aspects*, 2012, **400**, 67-72.

21. E. Kontturi, P. C. Thüne and J. W. Niemantsverdriet, *Langmuir*, 2003, **19**, 5735-5741.

22. D. Breitwieser, M. Kriechbaum, H. M. A. Ehmann, U. Monkowius, S. Coseri, L. Sacarescu and S. Spirk, *Carbohydrate Polymers*.

23. R. Giorgi, C. Bozzi, L. Dei, C. Gabbiani, B. W. Ninham and P. Baglioni, *Langmuir*, 2005, **21**, 8495-8501.

24. R. Giorgi, L. Dei, M. Ceccato, C. Schettino and P. Baglioni, *Langmuir*, 2002, **18**, 8198-8203.

25. P. A. Hassan, S. Rana and G. Verma, *Langmuir*, 2014, **31**, 3-12.

26. D. Fakin, N. Veronovski, A. Ojstršek and M. Božič, *Carbohydrate Polymers*, 2012, **88**, 992-1001.

27. D. Fakin, K. Stana Kleinschek, M. Kurečič and A. Ojstršek, *Surface and Coatings Technology*, 2014, **253**, 185-193.

28. K. Liu, Y. Xu, X. Lin, L. Chen, L. Huang, S. Cao and J. Li, *Carbohydrate Polymers*, 2014, **110**, 382-387.

29. in *Metallopolymer Nanocomposites*, Springer Berlin Heidelberg, 2005, vol. 81, pp. 65-113.

30. R. B. Grubbs, *Polymer Reviews*, 2007, **47**, 197-215.

31. Y. Liu, S. Z. D. Cheng, X. Wen and J. Hu, *Langmuir*, 2002, **18**, 10500-10502.

32. J. Jiang, G. Oberdörster and P. Biswas, *J Nanopart Res*, 2009, **11**, 77-89.

33. M. R. Kulterer, V. E. Reichel, R. Kargl, S. Köstler, V. Sarbova, T. Heinze, K. Stana-Kleinschek and V. Ribitsch, *Advanced Functional Materials*, 2012, **22**, 1749-1758.

34. S. Elzey and V. Grassian, *J Nanopart Res*, 2010, **12**, 1945-1958.

35. A. Mosca Conte, O. Pulci, A. Knapik, J. Bagniuk, R. Del Sole, J. Lojewska and M. Missori, *Physical Review Letters*, 2012, **108**, 158301.

36. M. Cristina Area and H. Cheradame, *BioResources*, 2011, **6**.

37. L. Taajamaa, E. Kontturi, J. Laine and O. J. Rojas, *Journal of Materials Chemistry*, 2012, **22**, 12072-12082.

38. M. Bracic, T. Mohan, R. Kargl, T. Griesser, S. Hribernik, S. Kostler, K. Stana-Kleinschek and L. Fras-Zemljic, *RSC Advances*, 2014, **4**, 11955-11961.

39. T. Mohan, S. Spirk, R. Kargl, A. Doliska, A. Vesel, I. Salzmann, R. Resel, V. Ribitsch and K. Stana-Kleinschek, *Soft Matter*, 2012, **8**, 9807-9815.

40. Presevation Technologies Website - Bookkeeper FAQ section. http://www.ptlp.com/fag.html (accessed Feb 25, 2015).

41. R. D. Smith, *Conservation of Library and Archive Materials and the Graphic Arts; Butteworth: London*, 1987.

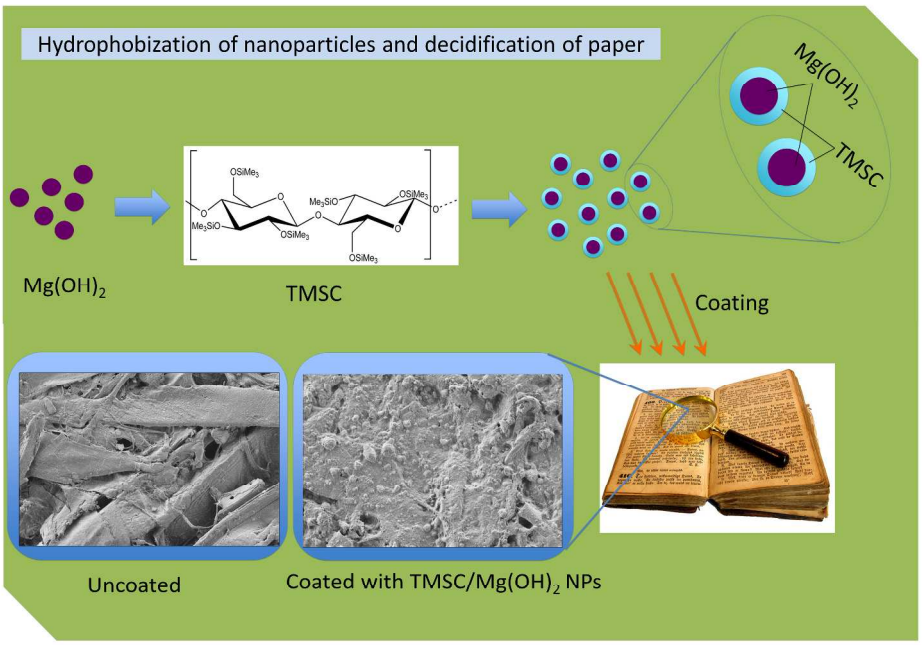

Graphical abstract
1200x840mm (96 x 96 DPI)